Submitted to ApJ Letters June 26, 2007
Preprint typeset using LaTeX style apjgalley

arXiv:0707.4676v2 [astro-ph] 4 Sep 2007

BLAZAR GAMMA-RAYS, SHOCK ACCELERATION, AND THE EXTRAGALACTIC BACKGROUND LIGHT

Floyd W. Stecker
Astrophysics Science Division, NASA Goddard Space Flight Center
Greenbelt, MD 20771, U.S.A.
stecker@milkyway.gsfc.nasa.gov

Matthew G. Baring and Errol J. Summerlin
Department of Physics and Astronomy MS-108,
Rice University, P.O. Box 1892, Houston, TX 77251, U.S.A.
baring@rice.edu, xerex@rice.edu

Submitted to ApJ Letters June 26, 2007

ABSTRACT

The observed spectra of blazars, their intrinsic emission, and the underlying populations of radiating particles are intimately related. The use of these sources as probes of the extragalactic infrared background, a prospect propelled by recent advances in TeV-band telescopes, soon to be augmented by observations by NASA's upcoming *Gamma-Ray Large Area Space Telescope (GLAST)*, has been a topic of great recent interest. Here, it is demonstrated that if particles in blazar jets are accelerated at relativistic shocks, then γ-ray spectra with indices less than 1.5 can be produced. This, in turn, loosens the upper limits on the near infrared extragalactic background radiation previously proposed. We also show evidence hinting that TeV blazars with flatter spectra have higher intrinsic TeV γ-ray luminosities and we indicate that there may be a correlation of flatness and luminosity with redshift.

Subject headings: gamma-rays: theory, (galaxies:) BL Lacertae objects: general, (cosmology:) diffuse radiation

1. INTRODUCTION

The comparison of theoretical models for the γ-ray spectra of blazars with observations is the standard approach used to understand the physical processes leading to their high energy emission. In the case of TeV components, the radiation models generally involve the synchrotron self-Compton (SSC) process. Determining the intrinsic emission spectra of such TeV sources requires that one account for the energy and redshift dependent absorption of γ-rays from these sources through $\gamma\gamma \rightarrow e^+e^-$ interactions with intergalactic photon backgrounds produced by stellar and dust emission. The cumulative background radiation seen at redshift $z = 0$ is commonly referred to as the extragalactic background light (EBL). Various calculations of extragalactic γ-ray absorption have been given in the recent literature and they are discussed along with the latest calculations in the paper of Stecker, Malkan & Scully (2006, hereafter SMS06).

The results given by SMS06 are based on two galaxy evolution models, *viz.* a baseline model (B) and a fast evolution model (FE). The spectral energy distributions of the extragalactic background light for these models are shown in Figure 1. The FE model is favored by recent *Spitzer* observations (Le Floc'h *et al.* 2005, Perez-Gonzalez *et al.* 2005). It provides a better description of the deep *Spitzer* number counts at 70 and 160μm than the B model. However, *GALEX* observations indicate that the evolution of UV radiation for $0 < z < 1$ may be somewhat slower and more consistent with the B model within errors (Schiminovich *et al.* 2005). And the 24μm *Spitzer* source counts are closer to the B model than the FE model.

Probing the EBL using blazar observations is contingent upon an accurate understanding of their emission spectra. Aharonian *et al.* (2006) have argued that intrinsic blazar spectra must have spectral indices $\Gamma_s \geq 1.5$. They use this assumption, together with *HESS* observations of the source 1ES 1101-232, to place an upper limit on the EBL of 14 nWm^{-2}sr^{-1} at a near infrared wavelength of 1.5 μm, corresponding to a frequency of 2×10^{14} Hz. As can be seen from both Figure 1 and Table 1, this value is consistent with model B, but not with the model FE, which is favored by the *Spitzer* observations. It is therefore important for exploring both galaxy evolution and blazar physics that we reexamine the assumption $\Gamma_s \geq 1.5$ made by Aharonian *et al.* (2006). This assumption has been questioned by Katarz'nski *et al.* (2006) in a different context, but we will examine it here in the light of the physics of shock acceleration, which provides insights into the distributions of underlying particle populations.

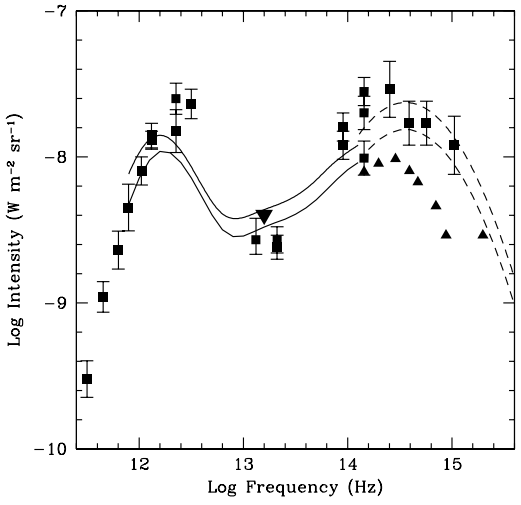

Fig. 1.— Spectral energy distribution of the EBL, taken from SMS06. Data points with error bars depict measurements, triangles show lower limits from source number counts, and the inverted triangle shows an upper limit from Stecker and De Jager (1997). The upper and lower solid curves depict FE (fast evolution) and B (baseline) model predictions. The dotted lines show the extensions of the models into the optical–UV (from SMS06).

TABLE 1
BLAZAR SPECTRAL INDICES IN THE 0.2 – 2 TEV ENERGY RANGE AND ISOTROPIC LUMINOSITIES AT 1 TEV

Source	z	Γ_{obs}	Γ_s (FE → B)	Γ_e (FE → B)	$\mathcal{L}$(1 TeV) [10^{36} W]
1ES 2344+514	0.044	3.0	2.5 → 2.6	4.0 → 4.2	2.9
Mrk 180	0.045	3.3	2.9 → 3.0	4.8 → 5.0	1.2
1ES1959+650	0.047	2.7	2.3 → 2.4	3.6 → 3.8	5.4
PKS 2005-489	0.071	4.0	3.4 → 3.5	5.8 → 6.0	8.6
PKS 2155-304	0.117	3.3	2.2 → 2.4	3.4 → 3.8	420
H 2356-309	0.165	3.1	1.5 → 1.9	2.0 → 2.8	200
1ES 1218+30	0.182	3.0	1.2 → 1.6	1.4 → 2.2	310
1ES 1101-232	0.186	2.9	1.0 → 1.5	1.0 → 2.0	230
1ES 0347-121	0.188	3.1	1.2 → 1.7	1.4 → 2.4	1200
1ES 1101+496	0.212	4.0	1.8 → 2.4	2.6 → 3.8	930

2. INTERGALACTIC ABSORPTION

The intergalactic γ-ray absorption coefficient (i.e. optical depth), $\tau(E, z)$, increases monotonically with energy and therefore leads to a steepening of the intrinsic source spectra as observed at Earth. SMS06 give a useful parametric form for $\tau(E, z)$ with the corrected parameters given in the erratum (Stecker, Malkan & Scully 2007). For sources at redshifts between 0.05 and 0.4, Stecker & Scully (2006, hereafter SS06) have shown that this steepening results in a well-defined increase in the spectral index of a source with an approximate power-law spectrum in the 0.2 – 2 TeV energy range with spectral index Γ_{obs}. This increase is a linear function in redshift z of the form $\Delta\Gamma = C + Dz$, where the parameters C and D are constants. The overall normalization of the source spectrum is also reduced by an amount equal to $exp\{-(A + Bz)\}$, again where A and B are constants. The values of A, B, C, and D are given for the B and FE models in SS06. SS06 have used this relation to calculate the intrinsic 0.2 – 2 TeV power-law γ-ray spectra of sources having known redshifts in the 0.05 – 0.4 redshift range for both the B and FE models of EBL evolution. A version of Table 2 of SS06 giving values for intrinsic spectral index of the source Γ_s is shown in Table 1. Table 1 also shows the respective indices $\Gamma_e = 2\Gamma_s - 1$ of the electron distributions in the sources under the assumption that the γ-rays are produced by inverse Compton interactions in the Thomson regime.

Using the formula derived in SS06, we can estimate the intrinsic "isotropic luminosity."[1] The isotropic luminosity of the blazar sources listed in Table 1 is obtained from the formula

$$\mathcal{L} \simeq 4\pi \frac{\Gamma_o - 2}{\Gamma_s - 2}(1+z)^{\Gamma_s - 2} F_o [d(z)]^2 e^{(A+Bz)} \qquad (1)$$

where d is the luminosity distance to the source, and F_o is its observed differential energy flux at 1 TeV. The other factors in the equation give the k-correction for the deabsorbed source spectrum and the normalization correction factor for absorption given in SS06. The observational references for the sources listed in Table 1 can be found in SS06 except for the new observations of 1ES 2344+514 (Albert *et al.* 2007a), 1ES 1959 + 650 (Albert *et al.* 2006), 1ES 0347-121 (Aharonian *et al.* 2007) and 1ES 1101+496 (Albert *et al.* 2007b). The source PG 1553+113 at $z = 0.36$ (included in Table 2 in SS06) is not listed here because the observations are in the energy range 0.09-0.6 TeV and are therefore below the operative energy range for applying the analytic approximation given in SS06. The blazars Mrk 421 and Mrk 501 are not included because their redshifts are significantly less than 0.05. However, these blazars are analysed by Konopelko *et al.* (2003).

The numbers given in the last column of Table 1 are derived for the fast evolution (FE) model. One may note that there appears to be a trend toward blazars having flatter intrinsic TeV spectra and higher isotropic luminosities at higher redshifts. However, one must be careful of selection effects. The TeV photon fluxes of these sources as observed by *HESS* and *MAGIC* only cover a dynamic range of a factor of ∼20. Therefore, only brighter sources can be observed at higher redshifts. This is because of both diminution of flux with distance, and intergalactic absorption (Stecker, de Jager & Salamon 1992). The observed $\mathcal{L}(z)$ trend is naturally expected in a limited population sample spanning a range of redshifts if the TeV-band fluxes are pegged near an instrumental sensitivity threshold. A more powerful handle on the intrinsic spectra and luminosities of these sources will be afforded by the upcoming *GLAST* γ-ray mission, with its capability for detecting many blazars at energies below 200 GeV.

3. PARTICLE DISTRIBUTIONS FROM SHOCK ACCELERATION

As discussed above, inferences of source spectra from specific blazars are contingent upon the particular choice of an EBL model. Hence there is significant uncertainty in deductions of the underlying distribution of emitting electrons in the case of SSC models, or protons in the case of hadronic models. It is a goal of this presentation to provide a cohesive connection between the particle distributions in blazars, the resulting emission spectra in the TeV band, and the spectrum of the EBL.

The rapid variability seen in TeV flares drives the prevailing picture for the blazar source environment, one of a compact, relativistic jet that is structured on small spatial scales that are unresolvable by present γ-ray telescopes. Turbulence in the supersonic outflow in these jets naturally generates relativistic shocks, and these form the principal sites for acceleration of electrons and ions to the ultrarelativistic energies implied by the TeV γ-ray observations. Within the context of this relativistic,

[1] We define isotropic here as if the source had an apparent isotropic luminosity even though blazars are highly beamed and their flux (and hence their apparent luminosity) is dramatically enhanced by relativistic Doppler boosting. This is similar to the nomenclature used for γ-ray bursts. The quantity $\mathcal{L}$ is equal to $4\pi\nu F_\nu$ given at hν = 1 TeV in units of 10^{36} W (10^{43} erg s^{-1}).

diffusive shock acceleration mechanism, numerical simulations are used here to derive expectations for the energy distributions of particles accelerated in blazar jets.

Diffusive acceleration at relativistic shocks is less well studied than that for nonrelativistic flows, yet it is the most applicable process for extreme objects such as pulsar winds, jets in active galactic nuclei, and γ-ray bursts. Early work on relativistic shocks was mostly analytic in the test-particle approximation (*e.g.*, Peacock 1981, Kirk & Schneider 1987, Heavens & Drury 1988), where the accelerated particles do not contribute significantly to the global hydrodynamic structure of the shock. A key characteristic that distinguishes relativistic shocks from their non-relativistic counterparts is their inherent anisotropy due to rapid convection of particles through and away downstream of the shock. This renders analytic approaches more difficult for ultrarelativistic upstream flows, though advances can be made in special cases, such as the limit of extremely small angle scattering (pitch angle diffusion) (e.g. Kirk & Schneider 1987; Kirk et al. 2000). Accordingly, complementary Monte Carlo techniques have been employed for relativistic shocks by a number of authors, including test-particle analyses for steady-state shocks of parallel and oblique magnetic fields by Ellison, Jones & Reynolds (1990), Ostrowski (1991), Bednarz & Ostrowski (1998), Baring (1999), and Ellison & Double (2004). It is such a simulational approach that is employed here to illustrate key spectral characteristics for particles accelerated to high energies at relativistic shocks that are germane to the blazar emission-EBL attenuation problem. For a recent discussion of relativistic shock acceleration, see Baring (2004).

The simulation used here to calculate diffusive acceleration in relativistic shocks is a Monte Carlo technique that has been employed extensively in supernova remnant and heliospheric contexts, and is described in detail in papers by Ellison, Jones & Reynolds (1990), Jones & Ellison (1991), Baring, Ellison & Jones (1994) and Ellison, Baring, & Jones (1996). It is conceptually similar to Bell's (1978) test particle approach to diffusive shock acceleration. Particles injected upstream gyrate in a laminar electromagnetic field, and particle trajectories are determined by solving a relativistic Lorentz force equation in the frame of the shock. Because the shock is moving with a velocity $\mathbf{u}$ relative to the plasma rest frame, there will, in general, be a $\mathbf{u} \times \mathbf{B}$ electric field in addition to the bulk magnetic field. Alfvén wave turbulence is modeled by using a phenomenological description of ion scattering in the rest frame of the plasma. The scattering allows particles to diffuse spatially along magnetic field lines, and to varying extent, across them as well. The scatterings are also assumed to be elastic, an assumption that is valid so long as the flow speed far exceeds the Alfvén speed. Hence, contributions from stochastic second-order Fermi acceleration, where the scattering centers move with the Alfvén waves, are generally neglected. The diffusion permits a minority of particles to cross the shock plane numerous times, gaining energy with each crossing via the shock drift and first-order Fermi processes.

A continuum of scattering angles, between large-angle or small-angle cases, can be modeled by the simulation. Denoting local fluid frame quantities by a subscript f, the time, δt_f, between scatterings is determined by the mean free path, λ_f, the speed of the particle, v_f, and the maximum scattering angle, $\theta_{\rm scatt}$, as derived in Ellison, Jones, & Reynolds (1990); for small angles, it is given by $\delta t_f = \lambda_f \theta^2_{\rm scatt}/(6v_f)$, a formula that generally holds to within 10% for $\theta_{\rm scatt} < 80^\circ$. Here λ_f is proportional to a power of the particle momentum p (e.g., see Ellison et al., 1990; Giacalone et al., 1992 for microphysical justifications for this choice), and for simplicity we assume that it scales as the particle gyroradius, r_g, i.e. $\lambda_f = \eta r_g \propto p$.

The parameter η in the model is a measure of the level of turbulence present in the system, coupling directly to the amount of cross-field diffusion such that $\eta = 1$ corresponds to the isotropic Bohm diffusion limit. It can be related to parallel ($\kappa_\parallel = \lambda_f v/3$) and perpendicular ($\kappa_\perp$) spatial diffusion coefficients through the relation $\kappa_\perp/\kappa_\parallel = 1/(1+\eta^2)$ (see Forman, Jokipii & Owens, 1974, Ellison et al., 1995, or Jokipii, 1987). In the parallel shocks considered here, where the **B** field is directed along the shock normal, η has only limited impact on the resulting energy spectrum, principally determining the diffusive scale normal to the shock. However, in oblique relativistic shocks, for which the field is inclined to the shock normal, the diffusive transport of particles across the field (and hence across the shock) becomes critical to retention of them in the acceleration process. Accordingly, for such systems, the interplay between the field angle and the value of η controls the spectral index of the particle distribution (e.g. see Ellison and Double, 2004; Baring, 2004).

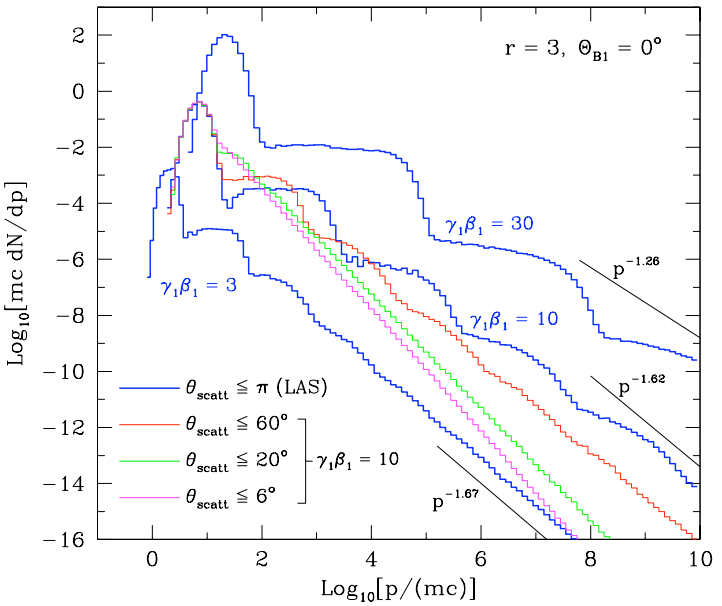

FIG. 2.— Particle distribution functions dN/dp from parallel ($\Theta_{\rm B1} = 0^\circ$), relativistic shocks of upstream-to-downstream velocity compression ratio $r = u_1/u_2 = 3$, as obtained from a Monte Carlo simulation of particle diffusion and gyrational transport. Three shock speeds $u_1 = \beta_1 c$ are depicted, namely $\beta_1 = 0.9487$, $\beta_1 = 0.995$ and $\beta_1 = 0.99944$, corresponding to the labels $\gamma_1\beta_1 = 3$, $\gamma_1\beta_1 = 10$ and $\gamma_1\beta_1 = 30$, respectively, on the heavyweight (blue) histograms. Scattering off hydromagnetic turbulence is modeled by randomly deflecting particle momenta by an angle within a cone, of half-angle $\theta_{\rm scatt}$, whose axis coincides with the particle momentum prior to scattering. The heavyweight (blue) lines are for the large angle scattering cases (LAS: $\theta_{\rm scatt} \le \pi \gg 1/\gamma_1$), and these asymptotically approach the power-laws $dN/dp \propto p^{-\Gamma_e}$ indicated by lightweight lines, at high and very high energies (not shown). For the $\gamma_1\beta_1 = 10$ case, also exhibited are three smaller angle scattering cases, $\theta_{\rm scatt} \le 60^\circ$ (red), $\theta_{\rm scatt} \le 20^\circ$ (green), and $\theta_{\rm scatt} \le 6^\circ$ (magenta) corresponding to pitch angle diffusion (PAD). These have high-energy asymptotic power-law indices of $\Gamma_e = 1.65$, $\Gamma_e = 1.99$ and $\Gamma_e = 2.20$, respectively.

Representative particle distributions that result from our simulation of diffusive acceleration at relativistic shocks are depicted in Figure 2, highlighting several key features. These distributions are equally applicable to electrons or ions, and so the mass scale is not specified. The spectral index declines and the distribution is flatter for faster shocks with larger upstream flow

(bulk) Lorentz factor γ_1 , when the velocity compression ratio r is fixed. This is a consequence of the increased kinematic energy boosting occurring at relativistic shocks. Such a characteristic is evident, for example in the work of Kirk & Schneider (1987), Ballard & Heavens (1991) and Kirk et al. (2000) for the case of pitch angle scattering, and Ellison, Jones & Reynolds (1990), Baring (1999) and Ellison & Double (2004) for much larger angle scattering. What is much more striking in Figure 2 is that the slope and shape of the nonthermal particle distribution depends on the nature of the scattering. The asymptotic, ultrarelativistic index of $\Gamma_e = 2.23$ is realized only in the mathematical limit of small (pitch) angle diffusion (PAD), where the particle momentum is stochastically deflected on arbitrarily small angular (and therefore temporal) scales. In practice, PAD results when the maximum scattering angle $\theta_{\rm scatt}$ is inferior to the Lorentz cone angle $1/\gamma_1$ in the upstream region. In such cases, particles diffuse in the region upstream of the shock only until their angle to the shock normal exceeds around $1/\gamma_1$. Then they are rapidly swept to the downstream side of the shock. The energy gain per shock crossing cycle is then roughly a factor of two, simply derived from relativistic kinematics (Gallant & Achterberg 1999; Baring 1999).

To contrast these power-law cases, Figure 2 also shows our results for large angle scattering scenarios (LAS, with $\theta_{\rm scatt} \sim \pi$), where the spectrum is highly structured and much flatter on average than p^{-2} . The structure, which becomes extremely pronounced for large γ_1 , is kinematic in origin, where large angle deflections lead to the distribution of fractional energy gains between unity and γ_1^2 in successive shock transits by particles. Gains like this are kinematically analogous to photon energy boosting by Compton scattering. Each structured bump or spectral segment shown in Figure 2 corresponds to an increment in the number of shock crossings, successively from $1 \to 3 \to 5 \to 7$ etc., as illustrated by Baring (1999); they eventually smooth out to asympotically approach power-laws that are indicated by the lightweight lines in the Figure. *The indices of these asymptotic results are all in the range* $\Gamma_e < 2$. Intermediate cases are also depicted in Figure 2, with $\theta_{\rm scatt} \sim 4/\gamma_1$. The spectrum is smooth, like the PAD case, but the index is lower than 2.23. Astrophysically, there is no reason to exclude such cases. From the plasma point of view, magnetic turbulence could easily be sufficient to effect scatterings on this intermediate angular scale, a contention that becomes even more salient for ultrarelativistic shocks with $\gamma_1 \gg 10$. It is also evident that a range of spectral indices is produced when $\theta_{\rm scatt}$ is of the order of $1/\gamma_1$, In this case, the scattering processes corresponds to a transition between the PAD and LAS limits.

Given the results of our numerical simulations, the implications for distributions of relativistic particles in blazars are apparent. There can be a large range in the spectral indices Γ_e of the particles accelerated in relativistic shocks, and these indices usually differ from $\Gamma_e \sim 2.23$. They can be much steeper, particularly in oblique shocks (e.g., Ellison & Double 2004; Baring 2004). However, they can also be much flatter, so that quasi-power-law particle distributions $p^{-\Gamma_e}$ with $\Gamma_e \leq 2$ are readily achievable. Such flat distributions from relativistic shock acceleration have not usually been admitted when considering properties of blazar jets and their possible emission spectra.[23]

4. CONCLUSIONS

This finding that relativistic shock acceleration produces particle spectra with a significant range of spectral indices, including those with $\Gamma_e \leq 2$ corresponding to inverse Compton γ-ray spectra with $\Gamma_s \leq 1.5$, has various consequences. The considerable diversity in the values Γ_e produced in relativistic shocks is matched by the diversity in the intrinsic spectral indices of blazars indicated in Table 1. Moreover, particle distributions with $\Gamma_e \leq 2$ are consistent with the inferred values for the three most distant blazars listed in the table. A hard TeV γ-ray spectrum with a value $\Gamma_s < 2$ within the context of SSC model building (see, *e.g.*, Stecker, De Jager & Salamon 1996), indicates that the energy range of the observation is below the Compton peak energy in the spectral energy distribution of the source, which is given by E^2 times the differential photon spectrum. For extreme blazars, this peak can easily be at an energy above 2 TeV (de Jager & Stecker 2002). A simple SSC model prediction then follows. The observation of an approximate power-law spectrum in the sub-TeV energy range should imply approximately the same index as the synchrotron emission in the optical to X-ray band.

Our reexamination of blazar γ-ray spectra in the light of relativistic shock acceleration theory has important implications for constraining the flux of the EBL in the near infrared. Specifically, the low values of $\Gamma_e \leq 2$ readily obtained in our numerical results implies an increase in the upper limit on the near infrared EBL to values above that obtained by Aharonian *et al.* (2006). Such a result is consistent with the fast galaxy evolution model which appears to be favored by the *Spitzer* observations.

Table 1 hints at a redshift evolution of TeV blazars with a trend toward flatter spectra and higher isotropic luminosities at higher redshifts. Although only ten blazars are listed in the table and selection effects are important, one may speculate as to whether there is a general trend in blazar activity in the form of higher jet Doppler factors at higher redshifts. Future combined *GLAST*-TeV broadband spectral data will further define intrinsic source properties, thus enabling the further investigation of possible redshift evolution of blazar flux and spectral characteristics. The *H.E.S.S.* and *MAGIC* atmospheric Čerenkov TeV telescopes have had remarkable success in observing blazars. With the *VERITAS* atmospheric Cherenkov telescope now online, the population of known TeV blazars will be extended considerably.

ACKNOWLEDGMENTS

We wish to thank the referee for helpful comments. MGB and EJS acknowledge the support of NASA through Grant No. NNG05GD42G and the National Science Foundation under Grant No. AST00-98705 for parts of this research.

[2]It has been suggested that electron distributions with $\Gamma_e < 2$ can be obtained by stochastic acceleration in combination with boundary layer particle trapping which produces a pileup effect (Ostrowsky 2000).

[3]Our results require the implicit assumption that the electron spectra produced during blazar flares are not significantly affected by cooling by synchroton radiation. This requires that $t_{acc} < t_{ccol}$ which constrains both the magnetic field strength and the electron energy (Baring 2002).

REFERENCES

Aharonian, F., *et al.* 2006, Nature 440, 1018.
Aharonian, F., *et al.* 2007, e-print arXiv:0708.302
Albert, J., *et al.* 2006, ApJ 639, 761.
Albert, J., *et al.* 2007a, ApJ 662, 892.
Albert, J., *et al.* 2007b, e-print arXiv:0706.4435 [astro-ph]
Ballard, K. R. & Heavens, A. F. 1991, Mon. Not. R. Ast. Soc. 251, 438.
Baring, M. G. 1999, in Proc. XXVI In tl. Cosmic Ray Conf. 4, 5., e-print astro-ph/9910128
Baring, M. G. 2002, Publ. Astr. Soc. Australia 19, 60.
Baring, M. G. 2004, Nucl. Phys. B 136C, 198., e-print astro-ph/0409303
Baring, M. G., Ellison, D. C. & Jones, F. C. 1994 ApJS 90, 547.
Bednarz, J. & Ostrowski, M. 1998, Phys. Rev. Letters 80, 3911.
Bell, A. R. 1978, Mon. Not. R. Ast. Soc. 182, 147.
De Jager, O. C. & Stecker, F. W. 2002, ApJ 566, 738.
Ellison, D. C. & Double, G. P. 2004, Astroparticle Phys. 22, 323.
Ellison, D. C., Baring, M. G., & Jones, F. C. 1995, ApJ 453, 873.
Ellison, D. C., Baring, M. G. & Jones, F. C. 1996, ApJ 473, 1029.
Ellison, D. C., Jones, F. C. & Reynolds, S. P. 1990, ApJ 360, 702.
Forman, M. A., Jokipii, J. R. & Owens, A. J. 1974, ApJ 192, 535.
Gallant, Y. A. & Achterberg, A. 1999, Mon. Not. R. Ast. Soc. 305, L6.
Giacalone, J., Burgess, D., & Schwartz, S. J. 1992, in ESA, Study of the Solar-Terrestrial System, 65.
Jokipii, J. R. 1987, ApJ 313, 842.
Le Floc'h, E.*et al.* 2005, ApJ 632, 169.
Heavens, A. F. & Drury, L. O'C. 1988, Mon. Not. R. Ast. Soc. 235, 997.
Jones, F. C. & Ellison, D. C. 1991, Space Sci. Rev. 58, 259.
Katarz'nski, K. *et al.* 2006, Mon. Not. R. Ast. Soc. 368, L56.
Kirk, J. G. & Schneider, P. 1987a, ApJ 315, 425.
Kirk, J. G., Guthmann, A. W., Gallant, Y. A., Achterberg, A. 2000, ApJ 542, 235.
Konopelko, A. *et al.* 2003, ApJ 597, 851.
Ostrowski, M. 1991, Mon. Not. R. Ast. Soc. 249, 551.
Ostrowski, M. 2000, Mon. Not. R. Ast. Soc. 312, 579.
Peacock, J. A. 1981, Mon. Not. R. Ast. Soc. 196, 135.
Pérez-González, P.G. *et al.* 2005, ApJ 630, 82.
Schiminovich, D. *et al.* 2005, ApJ 619, L47.
Stecker, F.W. & de Jager, O.C. 1997, in *Proc.Kruger Natl. Park Workshop on TeV Gamma-Ray Astrophysics* ed. O.C. de Jager (Potchefstoom: Wesprint), e-print astro-ph/971014
Stecker, F. W., de Jager, O. C. & Salamon, M. H. 1992, ApJ 390, L49.
Stecker, F. W., de Jager, O. C. & Salamon, M. H. 1996, ApJ 473, L75.
Stecker, F. W., Malkan, M. A. & Scully, S. T. 2006, ApJ 648, 774.
Stecker, F. W., Malkan, M. A. & Scully, S. T. 2007, ApJ 658, 1392.
Stecker, F. W. & Scully, S.T. 2006, ApJ 652, L9.